NUREG/CR-3773

Variation of Planetary Boundary Layer Dispersion Properties with Height in Unstable Conditions

Prepared by B. B. Hicks

Air Resources Laboratories
National Oceanic and Atmospheric Administration

Prepared for
U.S. Nuclear Regulatory
Commission

GPO Printed copy price: $4.00

NUREG/CR-3773
RB

Variation of Planetary Boundary Layer Dispersion Properties with Height in Unstable Conditions

Manuscript Completed: March 1984
Date Published: May 1984

Prepared by
B. B. Hicks

Air Resources Laboratories
National Oceanic and Atmospheric Administration
Oak Ridge, TN 37830

Prepared for
Division of Radiation Programs and Earth Sciences
Office of Nuclear Regulatory Research
U.S. Nuclear Regulatory Commission
Washington, D.C. 20555
NRC FIN B6333

ABSTRACT

Recent developments in surface boundary layer and planetary boundary layer meteorology are combined to evaluate the height dependency of the dispersion parameters σ_z and σ_y of the familiar Gaussian plume relationships. Recommendations are based on analyses of surface boundary layer data, such as are collected at industrial sites under existing NRC guidelines.

CONTENTS

LIST OF FIGURES

LIST OF TABLES

ACKNOWLEDGEMENTS

This report was prepared for the Earth Sciences Branch of the Office of Nuclear Regulatory Research, U. S. Nuclear Regulatory Commission, under Interagency Agreement NRC-01-79-012. This work is an extension of studies initiated by S. R. Hanna while he was associated with the Atmospheric Turbulence and Diffusion Laboratory. Dr. Hanna's extensive analyses of dispersion data and reviews of related literature greatly facilitated the completion of this project.

LIST OF SYMBOLS

A	Ratio of dispersion coefficients
c	Specific heat at constant pressure (cal $g^{-1}C^{-1}$)
C_f	Friction coefficient, u_*/u
d	Zero plane displacement (m)
F,f	Functions of controlling variables
f	Dimensionless frequency
f_m	Dimensionless frequency at the spectral peak
G,g	Functions of controlling variables
g	Acceleration due to gravity ($m\ s^{-2}$)
H	Sensible heat flux ($W\ m^{-2}$)
h	Effective emission altitude (m)
k	von Karman constant (0.4)
L	Monin-Obukhov scale length (m)
n	Natural frequency (s^{-1})
Q	Source strength ($kg\ s^{-1}$)
Ri	Richardson number $(g/\theta).(d\theta/dz)/(du/dz)^2$
Ri_b	Bulk Richardson number $(zg/\theta).\Delta\theta/u^2$
S	Spectral densities for u, v, w components (m^2s^{-1})
T	Temperature (C)
T_*	Temperature scaling parameter $H/\rho c_p u_*$ (C)
t	Time (s)
u,v,w	Velocity components along x,y,z axes ($m\ s^{-1}$)
u_*	Friction velocity ($m\ s^{-1}$)
w_*	PBL velocity scale $(ghz_i/\rho c_p\theta)^{1/3}$ ($m\ s^{-1}$)
x,y,z	Cartesian axes, x along the wind, y transverse, z vertical (m)

Y	$\ln(-z/L)$
z_i	Mixed layer depth (m)
z_o	Roughness length (m)
θ	Potential temperature (C) alternatively horizontal wind direction (rad)
θ_*	PBL temperature scale $T_*.u_*/w_*$ (C) Volumetric concentration (kg m^{-3})
ρ	Air density (kg m^{-3})
$\sigma_{u,v,w}$	Velocity standard deviations (m s^{-1})
$\sigma_{x,y,z}$	Plume dimension standard deviations (m)
$\sigma_{\theta,\phi}$	Wind direction standard deviations (rad)
ϕ	Vertical wind direction (rad)
ϕ_m	Wind gradient stability correction

ON THE VARIATION OF PBL DISPERSION PROPERTIES WITH HEIGHT IN UNSTABLE CONDITIONS

EXECUTIVE SUMMARY

Modern experiments on boundary layer meteorology are used as a basis for examining the variation of turbulence velocity statistics with height, stability, and surface roughness. Special attention is given to the possibility of spurious results arising from the use of inappropriate scaling methods.

Surface boundary layer behavior is studied using the data of the 1968 Kansas field experiment, which are interpreted in the light of the many other micrometeorological investigations conducted during the 1960's. These results are extended to above the surface boundary layer using the data of the 1973 Minnesota boundary layer experiment. The generality of conclusions drawn from these two land-based experiments is tested by comparing the results with observations of turbulence in the oceanic boundary layer, obtained over the Coral Sea.

In unstable conditions, the height variation of all velocity statistics is largely confined to the surface boundary layer, which constitutes the lowest 5 to 10% of the planetary boundary layer. Throughout most of the well-mixed layer, therefore, velocity component standard deviations can be expressed adequately in terms of external variables that scale the appropriate driving forces. In the case of the vertical velocity standard deviation, the controlling factors are the sensible heat flux and the depth of the mixed layer, which can be combined to define a convective scaling velocity that plays a role somewhat analogous to that of the friction velocity in surface boundary layer scaling. In the case of the horizontal velocity components, surface stress and stability appear to play the major roles. Values of the lateral and longitudinal velocity standard deviations are relatively constant above levels quite near the surface, corresponding to Ri (=z/L) approximately -0.3.

When converted to dispersion statistics suitable for initializing plume diffusion calculations, the role of surface stress is adequately incorporated by using conventional friction velocity scaling, with extrapolation through the mixed layer based on a height-varying friction coefficient. This friction coefficient is necessarily a function of both height and surface roughness, although both dependencies are rather slow. For horizontal dispersion, the stability variability of the friction coefficient is the sole stability influence of importance above the height $z = 3L$. For vertical dispersion, a further (multiplicative) dependence on the planetary boundary layer stability parameter $-z_i/L$ is indicated by the field data, in agreement with conventional meteorological wisdom.

1. INTRODUCTION

The questions most frequently asked by those who are interested in the fate and effect of emissions are (i) where are the emissions going, (ii) when are they going to arrive, (iii) how much are they being spread, and (iv) will concentrations at important downwind locations exceed some predetermined limit? For residents in areas likely to be affected, a similar set of questions arises: (i) what is the probability that air concentrations will be excessive, (ii) under what circumstances will the greatest air concentrations occur, and (iii) what remedial steps can be taken? A common thread running through all such discussions is the rate of atmospheric dispersion. A greatly dispersed plume will affect larger areas with somewhat smaller average concentrations than will a narrow "pencil" plume held in contact with the surface. On the other hand, increased vertical mixing causes greater coupling between plumes aloft and the surface. Thus the consequences of increasing dispersion rates are not trivial, but involve the interaction of several competing factors, any of which might be important in some specific instance.

All of these matters are discussed in the literature on atmospheric dispersion. Subjects such as fumigation, surface deposition, and effects of surface roughness are dealt with at length. The present purpose is not to compete with these discussions, but to consider in detail the role of altitude as a modifier of dispersion coefficients. Even this narrow subject has received considerable attention, both by dispersion meteorologists and by specialists on the structure and dynamics of the planetary boundary layer. Specialists in both areas are convinced that height variations can be important, but they differ as to the magnitude and formulation of the effect. The matter is not straightforward, since the usual method of analysis using nondimensionalized variables can lead to grossly misleading results, as will be seen later.

The present state of knowledge on turbulence statistics and dispersion coefficients in the atmospheric mixed layer is a consequence both of intensive case studies of PBL structure, and comprehensive investigations of the dispersion of tracer plumes. The former, reductionist studies are designed to provide basic information on the dynamic characteristics of the lower atmosphere, and to relate turbulence quantities to external properties; such as, synoptic-scale pressure fields, surface heating, and terrain roughness. In concept, the results of these studies permit a synthesis of the dispersion relationships provided by plume studies, and the plume studies provide opportunities to test what has been learned.

An excellent summation of the results of dispersion experiments has recently been presented by Horst et al. (1979). Likewise, Wyngaard (1980) has compiled papers describing the "state-of-the-art" regarding PBL parameterization. The material that follows draws heavily on these (and similar) compilations.

2. BACKGROUND

It is obviously impractical to develop a model to predict concentrations of airborne pollutants at every point in space and time. Rather, the plume can be described in a manner that mimics the probability density functions of Gaussian statistics. For a continuous emission at constant rate Q, the familiar near-field relationship describing plume behavior is

$$X = (Q/2\pi u\sigma_y\sigma_z) \cdot \exp\left[-(y^2/2\sigma_y^2) - (z-h)^2/2\sigma_z^2\right]. \qquad (2.1)$$

The exponential term is a shape factor that tends to unity at $y = 0$, $z = h$, the location of the source with an effective stack height h. The pollutant concentration modifier $(Q/2\pi u\sigma_y\sigma_z)$ is included to satisfy the requirement for conservation of pollutant mass at the source. In situations in which the plume intersects the ground, it is usual to assume a complete reflection at the surface, accounted for by a "mirror-source" term in Eq. 2.1:

$$X = (Q/2\pi u\sigma_y\sigma_z) \cdot \exp\left[-(y^2/2\sigma_y^2) - (z-h)^2/2\sigma_z^2 - (z+h)^2/2\sigma_z^2\right] \qquad (2.2)$$

Equations 2.1 and 2.2 describe the cross-sectional geometry of an average plume. Several fundamental questions arise immediately: what constitutes an appropriate averaging time, and how to allow for the effects of downwind distance, atmospheric stability, and surface roughness. Similarly, the influence of plume altitude must be examined. These various concerns interact in rather complicated ways. For example, it is difficult to separate the issue of altitude from that of stability, and neither can be considered independently of surface roughness. A related source of confusion arises from the frequent misapplication of surface boundary layer formulations to planetary boundary layer phenomena, and vice versa.

Studies of the dynamics of the lower atmosphere have progressed to the stage where stability parameterization is an accepted tool. Whereas much of the formative work in micrometeorology employed the gradient Richardson number, Ri, as a stability index, most recent work has used the quantity z/L. This dimensionless parameter originated from dimensional analysis; it is the non-dimensional grouping that results from combining the effects of the sensible heat flux H, surface friction velocity u_*, the height, and the buoyancy property g/θ (where g is the acceleration due to gravity and in this context θ is absolute potential temperature), into one parameter. In unstable (i.e. convective) conditions, z/L is negative and the relationships between fluxes and local gradients are such that z/L is numerically similar to Ri. In stratified flow, however, z/L and Ri are numerically quite dissimilar, although both take positive values.

The familiar "stability category" schemes for evaluating dispersion coefficients are the result of observation of plume behavior at heights in the range 10 to 200 m over grassland. Thus it must be expected that they might need some modification in order to represent dispersion at other altitudes, or over very rough (or very smooth) surfaces.

Typical Gaussian-plume dispersion models consider the plume cross-section characteristics σ_y and σ_z to be stability-dependent but invariant with height. However, micrometeorological research provides convincing evidence that stability varies strongly with altitude z. The common acceptance of the quantity z/L (where L is the Monin-Obukhov scale length of turbulence) as a favored micrometeorological stability index emphasizes the certainty associated with the height variability of stability itself and, by inference, of all quantities that are functions of stability. If the resulting height dependency extends to above the surface boundary layer, or if low-altitude sources are being considered, then this factor ought to be included in dispersion models.

In many simulations, stability is classified in a manner that does not permit easy quantification, as in the familiar "stability classes." The utility of this approach is evidenced by its popularity, yet its drawbacks are just as obvious. The question arises as to whether there is some height variability of the dispersion quantities that should be considered in models, but cannot now be readily included because of the limitations of the stability classification schemes.

Several authors have attempted to modify the usual dispersion modeling techniques to make use of micrometeorological stability parameters, usually z/L. Golder (1972), for example, related the A - F stability classes to surface roughness and z/L. More recently, Irwin, (1979) has extended this philosophy further by employing formulations derived for the planetary boundary layer (PBL) in a generalization of the usual dispersion schemes. Irwin's emphasis is on the application of relations developed between stability indices and other dimensionless properties of the unstable atmosphere, using L as a basic indicator of stability, but scaling according to the depth of the mixed layer, z_i, instead of z.

Some recent analyses of PBL turbulence data have tended to support arguments for including height-varying dispersion in daytime plume models. However, there is concern that analyses relating dimensionless turbulence characteristics to dimensionless stability indices (involving height) might be misleading, because of the manner in which the observed quantities are combined to produce the compound variables (q.v. height-variations of quantities like σ_y and σ_z, or alternatively σ_θ and σ_ϕ) that outwardly appear to be fairly well supported by analysis of dimensionless PBL quantities.

3. THE PHYSICS OF THE LOWER ATMOSPHERE

A basic characteristic of most of the earth's atmosphere is that it is stably stratified. Dynamic instability is a relative rarity, confined to the lowest part of the troposphere over much of the oceans and over land during most of the daylight hours. It is appropriate, therefore, to consider the evolution of the PBL (the planetary boundary layer, defined as that part of the lower atmosphere which responds directly to changes in surface roughness and heating), starting with its characteristic stable stratification at night.

Consider the case over land. As the atmosphere settles down overnight, the lowest few hundred meters stabilize most strongly. That is, the coldest, densest air is confined to layers nearest the surface. The potential temperature gradient $d\theta/dz$ is positive, and roughly constant over a considerable depth. Thus, in sufficiently stable stratification the temperature profile tends to linearity, on the average. The wind profile in such strongly stable conditions also approaches linearity, as can be argued on dimensional grounds, as follows. Stability is sufficient that air at some height is free to move without strong coupling to the surface. Thus, height can be eliminated from the list of parameters influencing the local wind gradient du/dz. Integration then leads directly to the prediction of a linear wind profile. In near-neutral conditions, profiles of both wind and potential temperature must approach a logarithmic form, so that a combination log-linear profile is usually assumed for intermediate stabilities.

The quiescent nature of the nocturnal stable atmosphere is disrupted at dawn, when insolation starts heating the surface. Heat provided by the sun is utilized in three major ways, to slowly heat the ground and its vegetative cover, to drive evaporation of liquid water available at the surface (via transpiration, usually), and to heat surface air. When surface air is sufficiently heated, convective cells start "bubbling" from the surface. These start eroding the stable temperature inversion near the surface. This convective activity generates a well-mixed layer whose depth is a result of the amount of sensible heat injected into it and the strength of the nocturnal inversion that the heat flux has to erode. All properties of the PBL are mixed by this process. Fine scale vertical wind structure is also destroyed. Figure 1 illustrates the general features of this behavior, using data obtained in the 1975 "Sangamon" study of PBL evolution (Hicks et al., 1981).

As the sun sets, radiative heating of the surface slowly decreases and surface cooling sets in. Sensible heat is drawn from the air, and a temperature inversion develops. As the inversion strengthens, turbulence levels decay until nearly-laminar flow develops. The increasing stability and decreasing turbulence intensities serve to reduce the surface momentum flux to a level at which air aloft is essentially free to move independently of surface frictional constraints. Winds in the PBL are then free to accelerate in response to large-scale inertial forces, but in the SBL periods of near-calm are typical. Plumes above the SBL will be carried for long distances with relatively little dispersion. However, the decoupling and the resulting acceleration of winds aloft causes wind gradients to slowly increase, forcing atmospheric stability to reduce until shear production of turbulence overcomes the stabilizing influence of the temperature gradient. A period of rapidly increased vertical mixing then occurs (a turbulent "burst"), which decreases wind and temperature gradients until the process commences again. This is an example of classical Kelvin-Helmholz instability. The consequences are evident in the surface boundary layer as infrequent outbreaks of turbulence, often referred to as turbulent intermittency.

The strong diurnal variability of mixed layer behavior that is associated with the heating and cooling cycle of land surfaces is not usually evident at sea. In essence, the thermal inertia of the oceans smoothes the daily cycle. There is no easily discernible daily variation in water surface temperature, and so the convective heating and radiative cooling cycles that drive much of the PBL evolution over land are missing, or at least are greatly moderated. On the average, heat is provided to the oceans by insolation, and hence the average condition is one of atmospheric instability in the lower troposphere. In this regard, the oceanic case of the PBL is an exception to the general rule that the atmosphere is stably stratified.

However, heat fluxes at sea are generally small, rarely exceeding 10% of values typical for daytime over land. It is sometimes claimed that the lower atmosphere should be near neutral stability, as a result. In reality, momentum fluxes are also often very small, and evaporating water tends to enhance instability (water vapor is buoyant). Near-neutrality is a rare occurrence at sea, as indeed is also the case over land.

The physical picture of convection leading to strong vertical mixing is of considerable relevance to questions concerning pollutant dispersion. Many reports have discussed the organized nature of convective cells in the mixed layer, with hexagonal patterns being evident in some near-perfect circumstances. These organized patterns develop above the surface boundary layer (or "constant-flux" layer), and the transfer mechanisms linking deep convection aloft with small-scale, random convection in the SBL are not yet clear. Several effects are obvious, however. Firstly, parts of plumes encountering the infrequent convective "chimneys" will be swept upwards, causing the familiar "looping plume" phenomenon. Secondly, parts of plumes not affected directly by convective updrafts will be subjected to the large-scale sinking motions imposed by continuity. Thus, the behavior of a plume in the convective mixed layer is not such that its meandering motions can be readily described in a simple, straightforward, Gaussian fashion, except as a description of the time-average. A non-buoyant plume should steadily sink, with intermittent updrafts forcing parts of it upwards to near the top of the mixed layer. As estimates, we can visualize updraft velocities of several meters per second, typically active over less than 10% of the area of interest, with a settling speed of many centimeters per second acting over the remaining area. A non-buoyant plume released at several hundred meters height in such circumstances might be expected to intersect the ground with maximum concentration about 20 to 60 minutes downwind, with complications arising because of the effects of infrequent updrafts.

The role of turbulence intermittency at night is difficult to assess. There have been few studies of plume dispersion at night, and those that have been conducted have been over sufficiently small distances that the infrequent but strong vertical mixing anticipated on the basis of Kelvin-Helmholz instability has not been well documented. It is accepted, however, that near-field plume dispersion coefficients are much less than in daytime, mixed conditions.

4. THE SURFACE BOUNDARY LAYER

4.1 SBL Relationships

The relationship between Gaussian dispersion statistics and turbulence quantities can be written as

$$\sigma_y = \sigma_v \cdot (x/\bar{u}) \cdot f(z, z_i, x, L, \text{etc.}) \tag{4.1}$$

and

$$\sigma_z = \sigma_w \cdot (x/\bar{u}) \cdot g(z, z_i, x, L. \text{etc.}) \tag{4.2}$$

(q.v. Hanna et al., 1977) where f and g are functions of the controlling variables. These functions are meant to represent relatively minor variations, after the first-order influences of x, u, and turbulence are accounted for by the preceding terms of the right hand side of Eqs. 4.1 and 4.2.

Initial dispersion is governed by local turbulence whose effect can be expressed in terms of the angular diffusion coefficients σ_θ and σ_ϕ:

$$\sigma_\theta = \sigma_v/u$$

and

$$\sigma_\phi = \sigma_w/u \tag{4.3}$$

It is this initial phase of plume development that is the major focus of this report.

It is convenient to consider the simple case f = g = 1, and to introduce stability effects for the surface boundary layer in the manner suggested by recent micrometeorological analyses. A few basic relations form the foundation. First, the logarithmic wind profile can be generalized as

$$u = (u_*/k) \cdot [\ln((z-d)/z_o) - \Psi_m(z/L)] \tag{4.4}$$

where Ψ_m is a correction function that depends only on the stability parameter z/L (or Ri). In unstable conditions, Ψ_m can be approximated by

$$\ln(\Psi_m) = 0.032 + 0.448Y - 0.132Y^2 \tag{4.5}$$

where $Y = \ln(-z/L)$. In stable conditions, Ψ_m takes the form of a simple proportionality:

$$\Psi_m = -5z/L; \qquad 0 < z/L < 1 \tag{4.6}$$

The precise form of Ψ_m in very stable conditions is not known; however, a linear wind profile is expected in the limit (see Hicks, 1976).

Equations 4.1, 4.2 and 4.3 relate dispersion statistics to turbulence properties; 4.4, 4.5 and 4.6 enable turbulence to be evaluated from external properties such as the velocity and surface characteristics, with a stability correction that is specified. To combine these various relations, it is usual to employ some form for the normalized turbulence statistics,

$$\sigma_v/u_* = F(z/L) \qquad (4.7)$$

and

$$\sigma_w/u_* = G(z/L) \qquad (4.8)$$

where F and G are functions that remain to be specified. It is then simple to eliminate the friction velocity from the above equations and to express the plume spreading quantities as

$$\sigma_y = kx\,[\ln(z-d)/z_o - \Psi_m]^{-1} \cdot F(z/L) \qquad (4.9)$$

and

$$\sigma_z = kx\,[\ln(z-d)/z_o - \Psi_m]^{-1} \cdot G(z/L) \qquad (4.10)$$

So far, the mathematics is well-founded, and follows much the same lines as many similar treatments (e.g. Chaudry and Meroney, 1973). Difficulties first arise when we attempt to determine the functions F(z/L) and G(z/L). Since the friction velocity is common to the expressions for both σ_u and z/L, highly misleading results can easily be obtained. Figure 2 (from Hicks, 1981) illustrates the difficulties that can arise. The "data" used to generate the diagram are all random numbers (listed in Table 1) selected only to fall into the expected overall ranges of values observed during the Kansas field experiment reported by Izumi (1971). The order that seems outwardly evident is in fact a misrepresentation of the true situation, since the original numbers used to create the figure were random. However, the curves drawn through the "data" averages are not adjusted to fit the "data"; the curves represent relationships extracted from the open literature. Thus, it seems that we should be careful about using many of the published and generally-accepted formulations describing turbulence statistics.

Figure 3 (also from Hicks, 1981) presents the results of an analysis of Kansas turbulence data, conducted in a manner designed to avoid the problems referred to above. The method of analysis makes use of independent measures of stability and normalized turbulence, in order to sidestep the problem of having the friction velocity appear on both axes of the plot, as in Figure 2. Figure 3 shows that the quantities σ_u/u_* and σ_v/u_* are not continuously increasing functions of atmospheric instability, as implied by the (random number) analysis of Figure 2 and by many common parameterizations of these terms. In reality, each of these normalized turbulence statistics increases rapidly from neutral through moderate instabilities, and attains a maximum value of about 2.0 at (and beyond) Ri = -0.4. Between neutral and Ri = -0.4, the dependence of σ_u/u_* and σ_v/u_* on Ri appears to be linear, rather than the power law relationship predicted by most other analyses based on z/L as a stability index. For unstable conditions, the behavior evident in Figure 3 can be summarized as

$$\sigma_u/u_* = 2.5 - 1.6Ri \;; \qquad -Ri < 0.3$$

$$\sigma_v/u_* = 1.9 - 3.5Ri \;; \qquad -Ri < 0.3$$

and

$$\sigma_u/u_* = \sigma_v/u_* = 3.0 \;; \qquad -Ri \geq 0.3 \qquad (4.11)$$

TABLE 1

Simulated turbulence data generated from random number tables. Values were constrained to lie in the ranges 10 to 30 C cm/s for sensible heat, 15 to 45 cm/s for friction velocity, 25 to 75 cm/s for vertical standard deviation, 60 to 180 cm/s for lateral, and 75 to 225 cm/s for longitudinal.

H	u_*	σ_w	σ_v	σ_u
29.3	30.1	56.9	108	183
10.9	27.3	53.4	131	146
13.2	20.2	54.9	166	89
23.3	35.3	28.3	88	180
16.5	40.9	68.4	95	150
27.2	18.3	32.5	66	109
21.3	32.8	44.0	178	158
25.2	15.2	69.5	89	128
17.6	31.0	49.4	82	85
15.2	43.4	72.0	162	159
26.1	33.7	66.6	64	110
27.5	30.7	28.6	121	224
18.4	23.7	26.5	118	188
26.1	19.1	35.9	97	215
19.2	16.7	34.3	61	81
27.4	41.1	39.9	79	80
21.5	24.9	69.8	79	158
19.5	40.3	44.4	157	198
21.5	26.0	62.5	98	119
28.3	41.3	38.0	179	196
14.8	41.4	55.3	92	173
22.8	15.8	63.1	67	214
18.2	15.1	30.8	155	216
20.2	37.2	50.1	151	75
17.8	38.2	72.6	152	146
13.5	36.5	58.6	126	206
24.9	24.6	73.8	90	196
27.5	44.6	38.8	80	196
27.8	24.6	46.0	91	214
24.0	22.9	51.3	113	138
16.0	34.2	71.0	145	148
12.5	42.3	26.9	70	136
27.8	19.2	45.3	74	191
13.0	25.9	42.9	100	129
15.9	24.8	62.9	170	115
21.0	28.5	35.1	168	83
22.9	22.9	56.5	146	83
13.0	33.9	61.3	143	200
18.1	23.6	38.5	84	190
12.5	35.4	45.5	122	143

Table 1 (con't)

H	u_*	σ_w	σ_v	σ_u
23.0	43.8	56.1	61	119
19.6	42.5	57.0	166	210
23.9	24.4	36.5	149	184
27.1	24.1	25.6	66	210
13.2	44.8	54.8	77	193
17.8	26.8	25.6	125	108
11.5	28.0	26.4	124	198
24.0	23.6	36.9	164	121
14.6	37.2	64.3	80	180
23.1	22.2	29.3	94	155

It is concluded that the familiar relationships that predict a monotonically increasing value for the quantities σ_u and σ_v with increasing instability are strongly influenced by the manner in which observations are combined to construct dimensionless quantities. Analysis of the Kansas data in a manner chosen specifically to avoid the cross-contamination problem fails to support the behavior usually associated with these same data, as represented by the curves drawn in Figure 2.

The lowest set of values plotted in Figure 3 represents the Kansas σ_w/u_* data. The dashed line is taken from the open literature, and is the same relationship drawn through the surrogate random data set of Figure 2. The line fails to fit the Kansas observations when the possibility of complex-variable contamination is avoided, even though the relationship that the line shows was originally derived from the same data (but using z/L as a stability index and hence introducing the sources of error that we are trying to avoid). However, it is obvious that the vertical velocity turbulence data behave quite differently from the horizontal data plotted in Figure 3 and discussed above; they do seem to increase monotonically in the manner expected by conventional micrometeorological thinking. Indeed, the form of the relationship is close to that which is frequently assumed:

$$\sigma_w/u_* = 1.1(1 - 2Ri)^{1/3} \quad . \tag{4.12}$$

It should be emphasized here that the present analysis assumes numerical equality between the indices Ri and z/L in unstable conditions, even though some workers question the accuracy of this assumption. The matter is not critical to this discussion.

4.2 Effects of Surface Roughness on SBL Dispersion

It is clear that surface roughness z_o plays a considerable part in determining diffusion rates and coefficients in the surface boundary layer. Equations 4.9 and 4.10, for example, illustrate the role of the micrometeorological roughness length as a factor for normalizing the height of observation near the surface. Later, the depth of the mixed layer, z_i, will be seen to play a similar part in the layers above the surface boundary layer. Table 2 lists roughness lengths and displacement heights d (q.v. Eqs. 4.9 and 4.10, once again) for a variety of fairly typical surfaces. Depending on the nature of the surface, roughness lengths can vary over more than three orders of magnitude.

Hanna et al. (1977) have suggested that the influence of roughness length can be incorporated in standard diffusion calculations by applying the simple correction

$$A = \sigma(z_o)/\sigma(10 \text{ cm}) = (z_o/10 \text{ cm})^{0.2} \tag{4.13}$$

to both vertical and transverse (lateral) components. The origin of this recommendation is evident in Figure 4, where the ratio A of the standard deviation (σ_y or σ_z) to the value appropriate if the surface roughness were 0.1 m is plotted against the surface roughness. The data are evaluated from relations Eqs. 4.9 and 4.10, assuming neutral stability and negligible zero plane displacement. The line drawn represents Eq. 4.13. The

TABLE 2

Roughness lengths typical of range of natural surfaces, and standard deviations of vertical velocity expected in 5 m/s winds. (From Kanemasu et al., 1979).

Surface	Approx. canopy height (m)	Roughness length (cm)	Neutral σ_w (cm/s)
Smooth ice		0.003	22
Ocean		0.005	23
Sandy desert		0.03	27
Tilled soil		0.1	31
Thin grass	0.1	0.7	39
Thick grass	0.1	2.3	49
Tall thin grass	0.5	5	57
Tall thick grass	0.5	10	67
Shrubs	1.5	20	82
Corn	2.3	30	92
Forest	10.0	50	113
Forest	20.0	100	162

fit seems acceptable; however, one might note that application of Eq. 4.13 to very smooth surfaces such as ocean or snow is likely to introduce some error. In such circumstances, it seems better to derive more accurate estimates of the correction factor A directly from the equations which led to the values plotted in Figure 4. Note also that the relations used to construct Figure 4 apply very near the surface; stability effects are ignored and will quickly become important as height increases above a few meters, especially at night. Moreover, the formulae only apply within the surface constant flux layer, which might not be more than a few tens of meters thick on some occasions. Thus, the recommended power law behavior with an exponent of 0.2 is an approximation that should be applied with some caution, even though gross errors appear unlikely if the relationships are used within the SBL.

5. THE PLANETARY BOUNDARY LAYER

5.1 PBL Relationships

The discussion given above is intended to demonstrate three major features of surface boundary layer turbulence data.

(1) The normalized vertical velocity standard deviation appears to increase continuously as instability increases, starting off with a neutral value of about 1.1 (rather than 1.3 or 1.35 proposed in earlier analyses).

(2) The normalized transverse velocity standard deviation increases rapidly with increasing instability over the range $0 > Ri > -0.3$, starting from about 1.7 at neutral and reaching a constant value of about 3.0 in strong instability.

(3) Although not discussed in detail here, the longitudinal velocity turbulence statistics appear to follow the behavior of the transverse, attaining much the same value in strong instability, although starting from a somewhat greater neutral value (about 2.5; see Figure 3).

It is known that stability increases with height. It remains to be seen how the various turbulence quantities relate to data obtained in the mixed layer, above the relatively shallow surface boundary layer.

Figure 5 shows the variation of velocity turbulence statistics with height alone through the depth of the mixed layer. The data are from the Minnesota turbulence experiment reported by Caughey et al. (1976). Following present-day convention, the altitude scale is normalized by the depth of the mixed layer at the time of the experiment. The quantifications of σ_u, σ_v, and σ_w are derived in as objective a manner as possible using the available observations. In every case, the values plotted are derived from the ratios of velocity standard deviations measured using a tethered sounding system to simultaneous tower-mounted observations of the same quantity, at 4 m height. Data were selected to lie in the altitude range between 10% and 90% of the depth of the mixed layer, so as to be above the effects of the surface, constant-flux while also being below the level

at which effects of free air entrainment at the top of the mixed layer become obvious. Throughout this rather deep layer of the lower atmosphere there is no marked increase in either σ_u or σ_v, both remaining close to the values observed at 4 m height. The vertical velocity statistic seems to be similarly constant with altitude, but it takes this constant value at some yet-undetermined level in the lowest 10% of the mixed layer.

A purist could easily point to the evidence in Figure 5 of a slight but consistent height variation of all three statistics, with maxima and minima at about $z/z_i = 0.4$. This is similar to the behavior found for σ_w by Warner (1972) for his Coral Sea data (yielding a maximum at $z/z_i \cong 0.3$), and is much as predicted by laboratory modeling studies (maximum at $z/z_i = 3.5$; Deardorff, 1970), but the variation is too small and the statistics are too uncertain for this to divert the present analysis.

Modern analyses of mixed layer evolution emphasize that the surface friction velocity is a less appropriate scaling quantity in the unstable PBL than the convective scaling velocity w_* (defined by $w_*^3 = gHz_i/\rho c_p \theta$; q.v. Deardorff, 1970: Tennekes, 1970). The matter appears to be of little relevance to the scaling of the horizontal velocity fluctuations, since these attain fairly constant values at moderate instabilities easily achieved very near the surface (see Figure 3) and then retain these values throughout the mixed layer (see Figure 5). The vertical component behaves quite differently, as would be expected on physical grounds. The major effect of additional buoyant energy would be expected to appear in the vertical velocity field. Inspection of Figure 3 shows this feature rather nicely; in fact, the diagram implies that eddies which are elongated along the wind near the surface in unstable conditions quickly become more circular in horizontal cross-section as height increases.

5.2 Effects of Surface Roughness on PBL Turbulence

The expressions given above for the relationships between velocity statistics in the surface boundary layer and micrometeorological variables identify a role for the surface roughness length z_o, as approximated by Eq. 4.13. The question arises as to whether any associated effects propagate into the PBL above the surface boundary layer. To investigate this matter, it is instructive to compare the Minnesota data used to construct Figure 5 with the Coral Sea observations reported by Warner (1972, 1973). Table 3 lists relevant data from the two experiments. As in the derivation of Figure 5, observations are confined to the height interval $0.1 < z/z_i < 0.9$, so as to be above the surface boundary layer while at the same time below the level of direct influence of the top of the mixed layer.

Table 4 summarizes the average conditions of the Minnesota and Coral Sea data sets, and presents the geometric mean values of turbulence statistics (and related quantities) derived from the observations. Even though the surface conditions of the two experiments were markedly different (summer continental grassland versus tropical ocean), there is no strong difference between the mean values of σ_w/w_*, this being the preferred form indicated by the considerations above. It should also be noted that the use of the friction velocity as a normalizing factor for vertical velocity variances

TABLE 3

Observations of σ_T (°C), σ_w (cm/s) and σ_v(cm/s) reported by Warner (1972, 1973) and by Izumi and Caughey (1976), with corresponding values of z (m), z_i (m), H (°C cm/s) and u_* (cm/s). Data are selected so that $0.1 < z/z_i < 0.9$. Note that there are substantial differences between the data sets. For the Coral Sea data, σ_T and H are calculated from virtual temperature information. No σ_u data are available for the Coral Sea, hence for the present purposes only the transverse velocity statistic σ_v will be considered.

Date and Identification	σ_T	σ_W	σ_v	z	z_i	H	u_*
Coral Sea							
26 June	.137	71	85	90	600	4.26	36
	.132	67	96	250	600	4.26	36
28 June	.136	65	92	90	650	3.61	36
	.127	66	84	250	650	3.61	36
29 June	.149	61	122	90	450	4.34	38
	.109	63	85	250	450	4.34	38
1 July	.136	51	90	90	570	3.36	32
	.132	58	81	250	570	3.36	32
	.127	54	75	400	570	3.36	32
3 July	.162	47	87	30	210	3.52	28
	.179	50	44	90	210	3.52	28
5 July	.088	58	64	90	490	2.30	18
	.099	51	65	250	490	2.30	18
6 July	.109	51	68	90	640	2.21	20
	.103	56	129	250	640	2.21	20
8 July	.139	70	112	90	830	5.08	32
	.133	88	132	250	830	5.08	32
	.132	87	112	400	830	5.08	32
	.129	85	159	550	830	5.08	32
11 July	.112	57	78	250	1100	2.87	32
	.123	55	83	400	1100	2.87	32
13 July	.094	45	54	90	670	1.80	24
	.083	49	55	250	670	1.80	24

Date and Identification	σ_T	σ_w	σ_v	z	z_i	H	u_*
Minnesota							
2A1	.17	124	139	914	1250	19.6	45
	.15	106	160	610	1250	19.6	45
	.18	93	143	305	1250	19.6	45
2A2	.19	110	188	1219	1615	20.9	45
	.15	129	192	914	1615	20.9	45
	.14	125	213	610	1615	20.9	45
	.20	103	166	305	1615	20.9	45
3A1	.11	140	229	610	2310	18.6	37
	.12	144	208	457	2310	18.6	37
	.13	127	190	305	2310	18.6	37
3A2	.10	124	184	610	2300	11.6	32
	.10	112	165	457	2300	11.6	32
	.11	99	148	305	2300	11.6	32
5A1	.06	67	108	610	1085	6.9	18
	.06	67	83	457	1085	6.9	18
	.07	71	90	305	1085	6.9	18
	.11	73	81	152	1085	6.9	18
6A1	.15	157	167	1219	2095	21.0	24
	.14	163	130	914	2095	21.0	24
	.15	145	158	610	2095	21.0	24
	.19	123	134	305	2095	21.0	24
6A2	.13	151	176	1219	2035	16.2	23
	.14	156	137	914	2035	16.2	23
	.14	125	157	610	2035	16.2	23
	.18	116	128	305	2035	16.2	23
6B1	.16	112	126	1219	2360	7.2	26
	.15	114	106	914	2360	7.2	26
	.13	103	117	610	2360	7.2	26
	.14	101	111	305	2360	7.2	26

Date and Identification	σ_T	σ_w	σ_v	z	z_i	H	u_*
7C1	.11	134	101	610	1020	22.1	28
	.12	133	92	457	1020	22.1	28
	.15	117	93	305	1020	22.1	28
	.26	115	101	152	1020	22.1	28
7C2	.10	121	103	610	1140	18.1	30
	.12	129	94	457	1140	18.1	30
	.14	113	83	305	1140	18.1	30
	.25	123	102	152	1140	18.1	30
7D1	.09	122	59	610	1225	9.9	25
	.10	131	93	457	1225	9.9	25
	.11	110	88	305	1225	9.9	25
	.16	125	97	152	1225	9.9	25

TABLE 4

Comparisons between geometric mean results obtained in the Coral Sea (C) and Minnesota (M) experiments.

		C	M	Ratio M/C
Number of Values		23	41	
σ_T	(°C)	0.1227	0.1316	1.07
	σ_T/T_*	1.0789	0.2621	0.24
	σ_T/θ_*	3.2124	1.7834	0.56
σ_w	(cm/s)	60.27	115.96	1.92
	σ_w/u_*	2.065	4.050	1.96
	σ_w/w_*	0.694	0.595	0.86
σ_v	(cm/s)	87.65	126.21	1.44
	σ_v/u_*	3.003	4.408	1.47
	σ_v/w_*	1.009	0.648	0.64
z	(m)	168.2	476.5	
z_i	(m)	594.4	1573.0	
H	(°C cm/s)	3.32	14.37	
u_*	(cm/s)	29.18	28.63	
f	(s^{-1})	4.14×10^{-5}	1.09×10^{-4}	
w_*	(cm/s)	86.89	194.81	
-z/L		3.06	39.12	
$-z_i/L$		10.83	129.1	
$-u_*/fL$		120.5	215.6	

in the PBL appears to be far less satisfactory. The matter is less clear in the case of the transverse component. For the ratios involving σ_v, the data of Table 4 are less convincing; however, we should note that the ratio observed over the ocean for σ_v/u_* was the same as is indicated by Figure 3, and that the Minnesota data differ by 47% on the average. Scaling by w_* in this instance does not decrease the apparent difference between the two experiments. It should be pointed out that experimental difficulties add to the uncertainty associated with these considerations; the Minnesota data were obtained using a tethered balloon system that may not have provided a sufficiently stable platform, and the Coral Sea data were obtained using an aircraft with potentially similar problems.

Temperature variances are also tabulated in Tables 3 and 4. In this case, scaling by the PBL quantity $\theta_* = H/(\rho c_p w_*)$ is far more appropriate than scaling according to the more familiar SBL quantity $T_* = H/(\rho c_p u_*)$. Once again, it is clear that buoyancy plays a dominant role in determining the variance in the convective PBL, much as was seen earlier for the case of the vertical velocity.

When considered in the light of the Kansas data of Figure 3, it appears that

(1) σ_v/u_* can be taken to be constant at 3.0 at all heights in the mixed layer above the level at which Ri = -0.3. (The Kansas and Coral Sea data agree well; the Minnesota experiment seems to be the odd man out.)

(2) σ_w/u_* increases monotonically with increasing instability through the surface boundary layer until it reaches a value such that σ_w/w_* is about 0.65 (the average of the two PBL results of Table 4), which value determines σ_w throughout the remaining depth of the unstable PBL.

(3) Once formulated in terms of the friction velocity and the convective scaling velocity, with appropriate stability dependencies in the surface boundary layer, there is no evidence of any further influence of surface roughness.

6. SPECTRA OF TURBULENCE

In the daytime, mixing in the lower atmosphere is strongly influenced by convection, especially in the vertical direction. Mechanically-generated mixing continues at all times, at rates that are controlled by wind gradients. Thus the stability-related differences between horizontal and vertical velocity variances (as evident in Figure 2, for example) are not unexpected; convection helps promote vertical mixing far more efficiently than horizontal mixing.

Low-frequency horizontal meandering is yet another cause of differences between vertical and horizontal mixing coefficients. The effect is clearly evident in velocity power spectra. Figure 6 summarizes the work of Kaimal et al. (1972), based on the exhaustive study of SBL turbulence conducted in Kansas in 1968 (Izumi, 1971). The dominance of low frequencies

in the lateral and longitudinal components in unstable conditions is obvious. In stable conditions, however, the velocity spectra seem to collapse back into a common shape, with similar peak frequencies for each of the lateral, longitudinal, and vertical components. Once again, this is as expected from the physics of the processes involved; the convective mechanism that enhances vertical motions rather than horizontal in unstable conditions is not present in stable. Figure 7 (also from Kaimal et al., 1972) shows the stability variation of the spectral peak frequencies, extracted from Figure 6. In stable conditions, the curves follow each other, with roughly a factor of two increase in peak frequency as we move from longitudinal (the slowest) to lateral, and then to vertical (the fastest) spectral components.

Peak frequencies for horizontal fluctuations are not illustrated for unstable conditions in Figure 7. Figure 6 shows these to be quite indeterminate. Examination of records of turbulence demonstrate the fundamental uniqueness of vertical velocity. In practice, convective activity is organized into irregular but relatively intense periods of updraft, separated by much longer quiescent periods of slow downdraft. Time series records (as in Figure 8) show that there are two time scales involved, corresponding to the characteristic length of each period of convective activity and to the characteristic spacing between them. When analyzed as in Figure 6, these two time scales combine to produce the appearance of a broad spectrum, stretching over a range of nondimensional frequencies extending from less than 0.001 to at least 10, and centered at about 0.1. The breadth of this spectrum is sometimes misinterpreted as implying that accurate data can only be obtained (and accurate predictions produced) if sensors and models can accommodate all frequencies over this range. In practice, this is not the case since very slow fluctuations in vertical velocity are essentially prohibited by the constraint of continuity and the appearance of important contributions by very slow fluctuations is little more than a consequence of an irregular "pulse repetition frequency" between convective cells.

On the other hand, the horizontal components are affected by no such constraint, and large-scale fluctuations in wind direction are indeed important. As a "rule-of-thumb," it has been suggested (Gifford, 1976) that the role of sampling time on evaluations of horizontal wind variance can be simplified to a relation much like Eq. 4.13:

$$\sigma_y(t)/\sigma_y(10 \text{ minutes}) = (t/10 \text{ minutes})^{0.2} \qquad (6.1)$$

(see also Hanna, 1982). The arguments presented above are summarized simply by Hanna: "The vertical component . . . does not need correction for averaging time, since large eddies are much less likely to occur in the vertical direction than in the horizontal direction."

However, it is unwise to dismiss the role of spectral differences too quickly. In the case of the vertical component, a much greater proportion of the variance is associated with high frequencies that will be completely ignored by any mechanical sensing device. Thus, the output of any sensor deployed for the purpose of obtaining vertical velocity and/or dispersion information cannot be applied directly in predictive models without correction

for high-frequency loss. The magnitude of the error will vary with the height of exposure, stability, and the characteristics of the sensor used. In neutral conditions, a sensor with a response length of the order of 2 m will frequently cause an underestimation of vertical dispersion coefficients by about 30% (see Tsvang et al., 1978, for an exhaustive examination of the effects of sensor characteristics on spectra). Horizontal characteristics are less affected in unstable conditions; however, it must be expected that data obtained at night will be substantially influenced for all wind components.

7. PBL DISPERSION

We have discussed how velocity standard deviations are related to dispersion coefficients in the lower atmosphere, and we have investigated selected alternative descriptions of the relationships with external variables such as surface fluxes and atmospheric stability. The presentation has been designed to show the extent of existing knowledge concerning the height and stability dependencies of PBL turbulence, and to emphasize the dangers that exist in the use of poorly selected dimensionless properties. In particular, the data show that daytime vertical dispersion in the mixed layer is almost entirely controlled by convection, so that scaling by the PBL convective scaling velocity w_* is especially appropriate. Above the SBL, there is no detectable role of surface friction in this particular instance. The limits normally associated with free convection appear to be readily attainable, and σ_w can be scaled accordingly. However, horizontal velocity fluctuations retain a memory of their tight link with the downward momentum flux.

This is in agreement with an attractively simple physical picture of mixed layer behavior. The convective lower troposphere behaves as a well-mixed slab of air, moving at a mean velocity determined by its two boundary constraints: large-scale flow aloft and surface friction below. Within this "slab," vertical mixing is a consequence of buoyancy which acts without much influence of the texture of the underlying surface. Momentum is easily transferred through this well-mixed layer; the concept of free convection carries with it no requirement for velocities to be very low, but only for convection to proceed without awareness of the mean flow of the fluid in which it is occurring.

The simple limit expressed by Eq. 4.11 for strongly unstable conditions leads to an equivalently simple relationship for the near-field crosswind dispersion coefficient σ_θ:

$$\sigma_\theta \cong 3.C_f, \qquad (7.1)$$

where C_f is the friction coefficient (u_*/u; the square root of the more familiar drag coefficient) that relates the surface friction velocity to the wind speed at the height of interest above the SBL. Likewise, the relationship between the vertical velocity standard deviation and the PBL convective scaling velocity (as evident in Table 4) can be re-arranged to show that the vertical dispersion coefficient σ_ϕ also depends on the friction coefficient, and on the PBL stability z_i/L as well:

$$\sigma_\phi = 0.65\ C_f \cdot (-z_i/L)^{1/3} \qquad (7.2)$$

Thus, in order to evaluate near-field Gaussian plume dispersion coefficients in any of their various forms, it is necessary to determine the friction coefficient appropriate for the height of interest, and to evaluate the stability parameter z_i/L. Note that the height dependence is contained solely within C_f, whereas the stability affects both C_f and $(-z_i/L)$. Note also that the height variability of C_f largely occurs within the SBL, the lowest 5 to 10% of the mixed layer. Evaluation of the dispersion coefficients therefore reverts to an analysis of SBL observations in order to evaluate L, estimation of the depth of the mixed layer z_i, and determination of the mixed layer friction coefficient C_f from the knowledge of surface roughness and stability.

8. INTERPRETATION OF TOWER DATA

8.1 Evaluating L from Surface Tower Data

Three factors impose severe limits on our ability to deduce accurate values of the Monin-Obukhov length scale from tower observations of wind and temperature gradients. First, the flux-gradient relationships that must be utilized in any such procedure are applicable only in steady-state, horizontally homogenous conditions, with negligible local variation in vertical fluxes or in any of the properties that might influence them. The magnitude of errors introduced as a consequence of departures from these ideal circumstances are largely unknown. Second, all data must be obtained at heights sufficiently far above the surface to be above the level of influence of individual surface roughness elements, while below a height typically 0.5% of the uniform upwind "fetch." (The size and effect of errors arising from poor site selection have not yet been addressed here.) Third, the uppermost level of tower measurement must be within the surface boundary layer, which is typically the lowest 5 to 10% of the convectively mixed layer.

These arguments suggest that it is wise to select observation sites with great care, and to make gradient measurements (for example) over as small a vertical interval as can be accomplished with the required accuracy using available equipment. However, a competing desire for data indicative of a wide area rather that some selected surface that may not be representative of the area as a whole must also be acknowledged. For this last reason, gradients are sometimes measured to heights well above the levels typical of careful micrometeorological work. It is required, therefore, to use these less-than-perfect data to deduce the meteorological fluxes that lead directly to a determination of L. In this case, there is no alternative but to apply micrometeorological flux-gradient relations (e.g. as recommended by Irwin and Binkowski, 1981), even though it must be anticipated that the basic data will rarely be obtained in the manner that is essential for accurate calculations. In part, this is a blessing, since it means that we need not be too concerned with the details of differences between alternative sets of flux-gradient relations, or similar fine points that are likely to be of great interest in other circumstances. We proceed, therefore, on the assumption that a limited set of perfect

data is available. As a minimum, this set will include observations of velocity and temperature at 10 m height, and velocity and temperature differences between 10 m and some greater height, often 30 or 60 m. Wherever possible, however, the analysis procedures will be selected to minimize the magnitude of possible errors associated with data inadequacies.

Dyer (1965) presents a conveniently simple yet well-founded method for evaluating sensible heat fluxes (H) from potential temperature gradients ($d\theta/dz$), without the need for extensive application of flux-gradient relations. The method is an application of surface boundary layer free convection theory, which results in a direct relationship between H, ($d\theta/dz$), the buoyancy paramenter (g/θ), and the height above the surface z, in conditions in which convection is unaffected by the friction velocity:

$$H/(\rho c_p) = H_*(g/\theta)^{1/2} (d\theta/dz)^{3/2} z^2 \qquad (8.1)$$

The dimensionless empirical constant H_* is 1.32 ± 0.06. Substitution of finite-difference values z_1 = 10 m, z_2 = 30 m (or alternatively 60 m), with the effective level of application taken to be the geometric mean height $z = (z_1.z_2)^{1/2}$, Eq. 8.1 simplifies to the convenient form

$$H/(\rho c_p) = 0.86(\theta(10) - \theta(30))^{3/2}$$

or alternatively

$$H/(\rho c_p) = 0.49(\theta(10) - \theta(60))^{3/2} \qquad (8.2)$$

Eqs. 8.2 were tested by Dyer, using data obtained in the surface boundary layer (of constant flux with height), for potential temperatures measured between 1 and 4 m, in which case the numerical constant was about 0.19. The relationship was found to provide an excellent determination of the sensible heat flux provided $z/L < -0.2$, with somewhat worse performance nearer neutral. In the application of main interest here, daytime instabilities at geometric mean heights above 20 m will almost always permit Eq. 8.2 to be applied with confidence that the stability constraint is satisfied. In the stability range $-0.2 < z/L < 0$, conditions are sufficiently near neutral that errors arising from the inappropriate application of Eqs. 8.2 are likely to have little practical consequence.

Determination of the Monin-Obukhov length scale L also requires knowledge of the friction velocity, u_*. The usual method of evaluating this quantity from wind and temperature gradient data is to apply micrometeorological flux-gradient relations such as those listed earlier (see Eq. 4.4 and 4.5) and to iterate on L if necessary. The assumption is made that both tower levels of velocity and temperature measurement are within a constant flux layer in equilibrium with the surface. Basing the analysis on velocity and temperture differences maximizes the sensitivity to errors arising from site imperfections and surface irregularities. Thus it is preferable to avoid this technique whenever the micrometeorological quality of the site or the data is not assured. In the case of the temperature data considered above, the matter is sidestepped by using free convection

relationships that require no velocity information. In the case of the friction velocity, the sensitivity to errors can be minimized by using friction coefficient relationships applied to single velocity measurement at the lowest level. In this way, the sensitivity to errors in evaluating stability is considerably reduced, and the possibility of propagating errors arising from incorrect gradient data is completely avoided.

Table 2 lists the roughness lengths associated with a wide range of natural surfaces. Since this quantity appears in a logarithmic term in the determination of C_f (see Eq. 4.4) finer resolution and greater accuracy are probably not required. Care should be taken, however, to use a value of the roughness length that is appropriate for the height of the wind data being interpreted. The value should be an average over an upwind distance extending out to about 100 times the height of observation.

The recommended procedure is as follows:

(1) Evaluate H from the potential temperature gradient data, using Eqs. 8.1 or 8.2.

(2) Estimate u_* from the wind speed measured at 10 m (or below), using a friction coefficient derived as u_*/u from Eq. 4.4 by assuming some likely value for u_* (say 10% of the wind speed) to make a first estimate of L.

(3) Iterate on u_* until satisfactory convergence is achieved. In practice, it has been found that any of the usual schemes for guiding the iteration procedure will produce rapid convergence.

Since the sensible heat flux and the friction velocity are uniquely determined by the temperature gradient and the wind speed, it is possible (and very convenient) to produce graphs or tables relating the two sets of quantities. For any given roughness length and height of observation, the stability property z/L is determined by the bulk Richardson number

$$Ri_b = (zg/\theta)\cdot(\theta(z_2) - \theta(z_1))/u^2 \qquad (8.3)$$

(see Irwin and Binkowski, 1981). Once z/L is known, subsequent steps are relatively straightforward.

At alternative procedure relates z/L directly to the unstable gradient Richardson number, evaluated at

$$Ri = (g/\theta)\cdot(z_2 - z_1)\cdot(\theta(z_2) - \theta(z_1))/(u(z_2) - u(z_1))^2 \qquad (8.4)$$

In this way, the need for estimating the surface roughness length is avoided, but much greater importance is associated with the meteorological quality of the site because of the need to employ velocity differences rather than the velocities themselves.

8.2 Estimating C_f for the Mixed Layer

Considerable attention has been paid by experimentalists and modelers alike to the question of turbulence and turbulent fluxes in the planetary boundary layer. The matter of mean flow conditions remains less well understood. To a considerable extent, this relatively poor understanding is a consequence of the lack of suitable instrumentation by which wind speeds aloft can be monitored over extensive periods. Most available data comes from analyses of balloon ascents, which are essentially "snapshots" of a highly turbulent layer of the atmosphere in which relatively small mean gradients might be embedded.

One of the most extensive bodies of high-quality PBL data is the "Wangara" experiment reported by Clarke et al. (1971). This data set provides an extensive set of hourly balloon ascent data, extending over approximately forty days. Analyses of these data have been limited somewhat by the lack of a companion set of SBL data, especially on sensible heat and momentum fluxes. Recently, a compilation of such data has been completed (Hicks, 1981). By combining the two sets of information, some improved information on the variation of C_f with height and stability in the mixed layer can be obtained.

Figure 9 shows the stability dependence of the residual friction coefficient derived directly from observations of wind speed at altitudes of 50, 100, 500, and 1000 meters, and from friction coefficients obtained from completely independent surface boundary layer data. Values of friction coefficients have been grouped according to stability, expressed (for reasons of convenience in showing the results) as -1/L. Friction coefficients have been corrected for the simple variation predicted by an extension of the neutral-stability logarithmic wind profile, so that the quantities that are plotted can be viewed as increments that would be appropriate if SBL formulations were applicable throughout the mixed layer in neutral stability. In fact, this procedure provides a simple method for collapsing data at the different heights into a single straight line. To a first approximation, it seems adequate to assess the height variation of the average mixed layer friction coefficient by means of a simple logarithmic form, and to impose an additive stability correction that is independent of height. It must be emphasized that this procedure cannot be expected to apply well in the surface boundary layer, where the accuracy and relevance of alternative relations is well known. The result is intended to apply through the bulk of the mixed layer, above the SBL. It must also be noted that the value of the roughness length used in deriving Figure 9 is 1 cm, which is indicative of the general area of the Wangara central site but not of the immediate vicinity of the SBL towers. These considerations lead to a conveniently simple relationship for the friction coefficient as a function of altitude and stability:

$$C_f = k/\ln((z-d)/z_o) - 0.085/L \qquad (8.5)$$

for L in meters. Several points about this relationship need to be emphasized further. In particular, it is an empirical expression whose relationships with theoretical and modeling results remains to be explored. Further, it omits z as a major controlling factor; while this omission is likely to be erroneous, the significance of the assumption is yet to be ascertained. Finally, the expression is derived from only one set of observations, and tests against other sets of data must be carried out.

9. SUMMARY AND RECOMMENDATIONS

Many of the relationships advocated in published examinations of the roles of stability and mixed-layer properties on turbulence in the PBL have been adversely influenced by statistical interactions between variables. An analysis of data structured to avoid such problems confirms that the convective scaling velocity w_* is an appropriate factor to consider in formulations of vertical dispersion, but is less relevant in the case of horizontal dispersion. In the surface boundary layer, which is the lower 5 to 10% of the mixed layer, conventional relationships appear to work quite well, provided appropriate corrections are made for the effects of statistical "contamination" referred to above.

The surface boundary layer properties H and u_* are critical intermediates in any evaluation of mixed layer dispersion. These terms can be derived from tower observations, but considerable care must be taken with the exposure of the instruments, the quality of the site, and the interpretation of gradient data. In general, vertical differences of any micrometeorological quantity are greatest nearest the surface, and values obtained become increasingly difficult to measure and interpret as height above the surface increases.

Once H and u_* are known, mixed layer dispersion quantities can be estimated by using relatively simple formulae involving the friction coefficient appropriate for the height of interest and the PBL stability index z_i/L. Values of the friction coefficient can be derived from knowledge of the surface roughness length and the Monin-Obukhov scale length, L. At present, however, such methods remain fairly poorly understood, and the simple relationships presented here should be used with some caution.

The step-by-step procedure that is recommended for unstable conditions is as follows:

(1) Determine the roughness length by inspection of the site and comparison with Table 2. The value used should be appropriate for the surface that influences the observed wind, and may be a function of wind direction if the site is not horizontally uniform. The roughness length can be determined in advance; it is not a rapidly varying quantity. All other steps in this sequence require the use of time-evolving data.

(2) Determine the depth of the mixed layer, z_i, using either some direct-measurement technique (sodar, lidar, radiosondes, tethersondes, etc.) or some alternative parameterization scheme. This quantity does not need to be evaluated with precision unless it is feared that plume rise might bring emissions into immediate contact with the upper boundary of the mixed layer.

(3) Estimate the surface heat flux from tower potential temperature gradients, using the free-convection approximation.

$$H/(\rho c_p) = C(\theta(z_1) - \theta(z_2))^{3/2}$$

where the constant C is about 0.86 for temperatures measured at z_1 = 10 and z_2 = 30 m, and 0.49 for measurements at 10 and 60 m (see Eqs. 8.1 and 8.2).

(4) Estimate the friction velocity from the wind speed measured at 10 m height, using the roughness length evaluated in step 1 and assuming the applicability of the simplified friction coefficient formulation given as Eq. 8.5:

$$u_* = (ku)/\ln((z-d)/z_o) - 0.085\ u/L.$$

Note that the Obukhov length scale L (in meters) is defined as

$$L = - u_*^3\theta/kg(H/\rho c_p)$$

where the heat flux H is in W m^{-2}, and where $(H/\rho c_p)$ is in °C m/s.

Once an estimate of u_* is obtained, it can be refined by iteration or by application of the more precise micrometeorological formulation expressed by Eq. 4.4, with stability corrections introduced using Eq. 4.5. It should be emphasized that evaluation of the friction velocity by interpretation of wind gradient data obtained between typical levels (10 and 30 m, or 10 and 60 m) is specifically not recommended, since this kind of analysis requires site uniformity and data quality that are exceedingly rare. However, methods making use of the bulk Richardson number (q.v. Eq. 8.3) have the special attraction that they permit a direct evaluation of stability without the need for iteration. The necessary relationships can be summarized in advance, in tabular or graphical form, once the roughness characteristics of the site are known.

After the sensible heat flux, the friction velocity, and the depth of the mixed layer are evaluated, estimates of dispersion quantities can be derived easily.

(5) Evaluate velocity standard deviations on the assumption that SBL formulations apply at the altitude of interest, z. Equations 4.11 and 4.12 provide the basis for evaluation.

$$\sigma_u = u_*(2.5 - 1.6z/L) \quad ; \quad -z/L < 0.3$$

$$\sigma_v = u_*(1.9 - 3.5z/L) \quad ; \quad -z/L < 0.3$$

$$\sigma_u = \sigma_v = 3.0u_* \quad ; \quad -z/L \geq 0.3$$

$$\sigma_w = 1.1u_*(1 - 2z/L)^{1/3}$$

Here, the stability indices z/L and Ri have been assumed to be equal in unstable stratification.

(6) If z is greater than $z_i/10$, then the estimate of the vertical velocity standard deviation derived above should be replaced by the PBL estimate based on convective scaling:

$$\sigma_w = 0.65(gHz_i/\rho c_p \theta)^{1/3}$$

Note that σ_w is a slowly-varying function of height and that uncertainties about which formulation is best to apply near the hand-over height between u_*- and w_*- scaling is unlikely to have severe practical consequences.

(7) If angular dispersion coefficients are required, then these can be evaluated directly from estimates of the friction coefficient appropriate for the altitude z:

$$C_f = k/\ln((z-d)/z_o) - 0.085/L$$

$$\sigma_\theta = 3.C_f$$

$$\sigma_\phi = (C_f/u_*).\ \sigma_w$$

All of these relationships are derived as empirical approximations to boundary layer relationships that are still under development. It must be expected that considerable improvements will take place as the quantity of high-quality data expands. There are several circumstances in which the approximations given here will probably prove to be inadequate. In particular, over water the specification of roughness length is known to be velocity dependent, and the stability index should then include an evaporative component. In so-called complex terrain (e.g. coastlines, mountains, lakes, etc.), the present formulations are almost certainly deficient because they omit consideration of gross streamline modification due to the presence of individual surface features.

10. REFERENCES

Chaudry, F. H., and R. N. Meroney, "Similarity Theory of Diffusion and the Observed Vertical Spread in the Diabatic Surface-Layer," Boundary-Layer Meteorology 3, 405-415 (1973).

Clarke, R. H., A. J. Dyer, R. R. Brook, D. G. Reid, and A. J. Troup, "The Wangara Experiment: Boundary Layer Data," Technical Paper Number 19, CSIRO Division of Meteorological Physics, Aspendale, Victoria, Australia, 362 pp. (1971).

Deardorff, J. W., "Convective Velocity and Temperature Scales for the Unstable Planetary Boundary Layer and For Rayleigh Convection," Journal of the Atmospheric Science 2, 1211-1213 (1970).

Doran, J. C., T. W. Horst, and P. W. Nickola, "Experimental Observations of the Dependence of Lateral and Vertical Dispersion Characteristics on Source Height," Atmospheric Environment 12, 2259-2263 (1978).

Dyer, A. J., "The Flux-Gradient Relation for Turbulent Heat Transfer in the Lower Atmosphere," Quarterly Journal of the Royal Meteorological Society 91, 151-157 (1965).

Gifford, F. A., "Turbulent Diffusion Typing Schemes - A Review," Nuclear Safety 17, 68-86 (1976).

Golder, D., "Relations Among Stability Parameters in the Surface Layer," Boundary-Layer Meteorology 3, 47-58 (1972).

Hanna, S. R., G. A. Briggs, J. Deardorff, B. A. Egan, F. A. Gifford, and F. Pasquill, "AMS Workshop on Stability Classification Schemes and Sigma Curves -- Summary of Recommendations," Bulletin of the American Meteorological Society 58, 1305-1309 (1977).

Hicks, B. B., "Wind Profile Relationships From the Wangara Experiment," Quarterly Journal of the Royal Meteorological Society 102, 535-551 (1976).

Hicks, B. B., "Some Limitations of Dimensional Analysis and Power Laws," Boundary-Layer Meteorology 14, 567-569 (1978).

Hicks, B. B., "An Examination of Turbulence Statistics in the Surface Boundary Layer," Boundary-Layer Meteorology 21, 389-402 (1981).

Hicks, B. B., "An Analysis of Wangara Micrometeorology: Surface Stress, Sensible Heat, Evaporation, and Dewfall," 36 pp. NOAA Technical Memorandum ERL ARL-104, 1981, available from Atmospheric Turbulence and Diffusion Laboratory, Post Office Box E, Oak Ridge, Tennessee 37830.

Hicks, B. B., G. D. Hess, M. L. Wesely, T. Yamada, P. Frenzen, R. L. Hart, D. L. Sisterson, P. E. Hess, F. C. Kulhanek, R. C. Lipschutz, and G. A. Zerbe, "The Sangamon Field Experiments: Observations of the Diurnal Evolution of the Planetary Boundary Layer Over Land," 175 pp. Argonne National Laboratory Report ANL/RER-81-1, (1981).

Horst, T. W., J. C. Doran, and P. W. Nickola, "Evaluation of Empirical Atmospheric Diffusion Data," 135 pp, USNRC Report NUREG/CR-0798, PNL-2599, 1979. Available for purchase from National Technical Information Service, Springfield, Virginia 22161

Irwin, J. S., "Estimating Plume Dispersion -- a Recommended Generalized Scheme," pp. 62-69 in Preprints, Fourth Symposium on Turbulence, Diffusion, and Air Pollution, American Meteorological Society, Boston, Massachusetts 02108, (1979).

Irwin, J. S., and F. S. Binkowski, "Estimation of the Monin-Obukhov Scaling Length Using On- Site Instrumentation," Atmospheric Environment 15, 1091-1094 (1981).

Izumi, Y., "Kansas 1968 Field Program Data Report," 69 pp, Air Force Cambridge Research Laboratories Environmental Research Papers No. 379, AFCRL-72-0041, 1971. Available for purchase from National Technical Information Service, Springfield, Virginia 22161

Izumi, Y., and J. S. Caughey, "Minnesota 1973 Atmospheric Boundary Layer Experiment Data Report," 28 pp, Air Force Cambridge Research Laboratory Environmental Research Papers, No. 547, AFCRL-TR-76-0038 1976. Available for purchase from National Technical Information Service, Springfield, Virginia 22161

Kaimal, J. C., J. C. Wyngaard, Y. Izumi, and O. R. Cote, "Spectral Characteristics of Surface-Layer Turbulence," Quarterly Journal of the Royal Meteorological Society 98, 563-589 (1972).

Kanemasu, E. T., M. L. Wesely, B. B. Hicks, and J. L. Heilman, "Techniques for Calculating Energy and Mass Fluxes," Chapter 3.2, pp. 156-182. In Modification of the Aerial Environment of Crops. (Americam Society of Agricultural Engineering, St. Joseph, Michigan 1979).

Tennekes, H., "Free Convection in the Turbulent Ekman Layer of the Atmosphere," Journal of the Atmospheric Sciences 27, 1927-1934 (1970).

Tsvang, L. R., B. M. Koprov, S. L. Zubkovskii, A. J. Dyer, B. B. Hicks, M. Miyake, R. W. Stewart, and J. W. McDonald, "A Comparison of Turbulence Methods by Different Instruments; Tsimiyansk Field Experiment 1970," Boundary-Layer Meteorology 3, 499-521 (1973).

Warner, J., "The Structure and Intensity of Turbulence in Air Over the Sea," Quarterly Journal of the Royal Meteorological Society 98, 175-186 (1972).

Warner, J., "Spectra of the Temperature and Humidity Fluctuations in the Marine Boundary Layer," Quarterly Journal of the Royal Meteorological Society 99, 82-88 (1973).

Wyngaard, J. C., (Ed.), "Workshop on the Planetary Boundary Layer," in Proceedings of American Meteorological Society Workshop, 14-18 August 1978, Boulder, Colorado (1980).

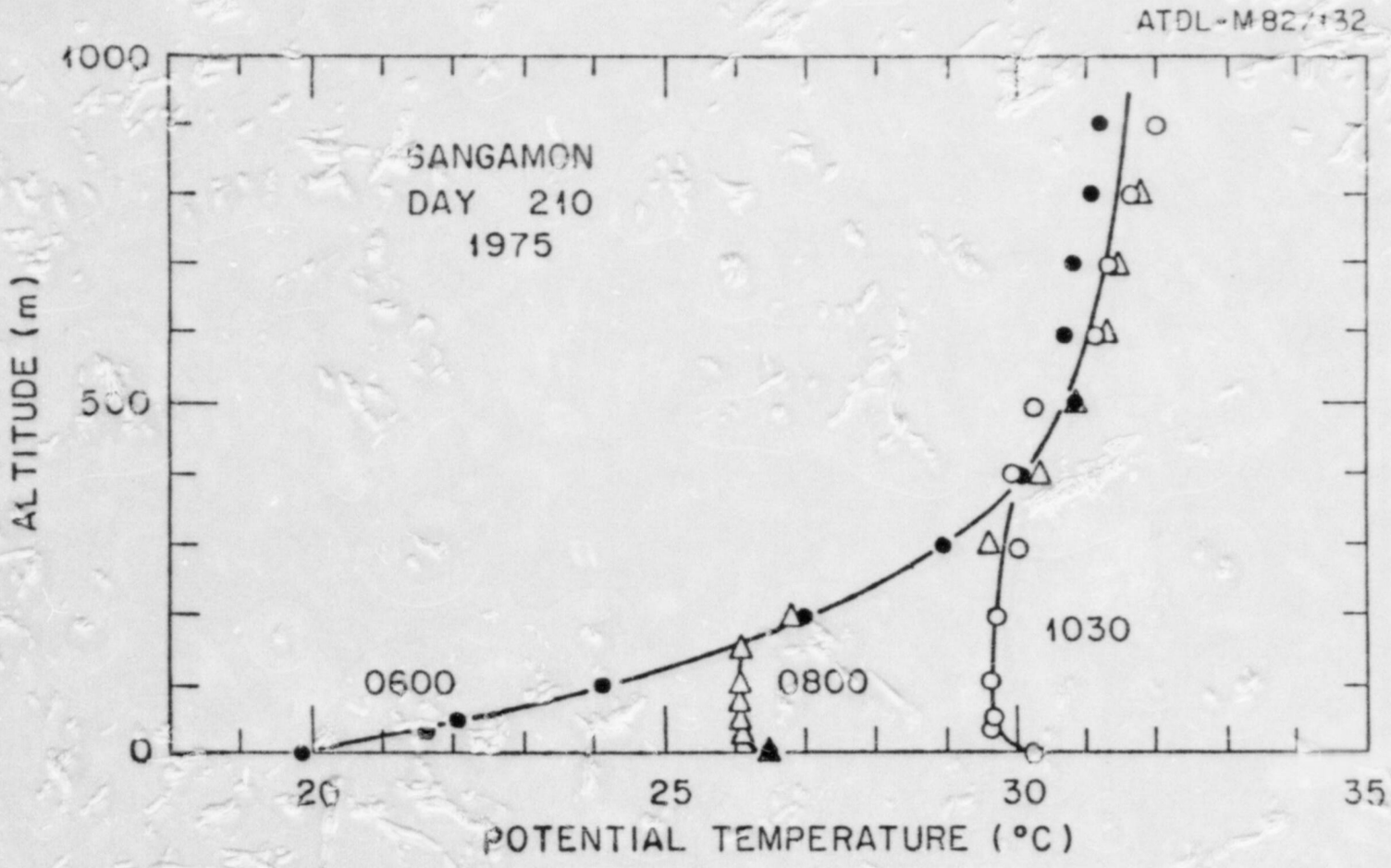

Figure 1 A sequence of three potential temperature profiles measured during the 1975 "Sangamon" study in central Illinois, showing the gradual erosion of the predawn temperature inversion. At 0800, the convectively well-mixed layer had grown to about 150 m. At 1030, it was about 400 m deep.

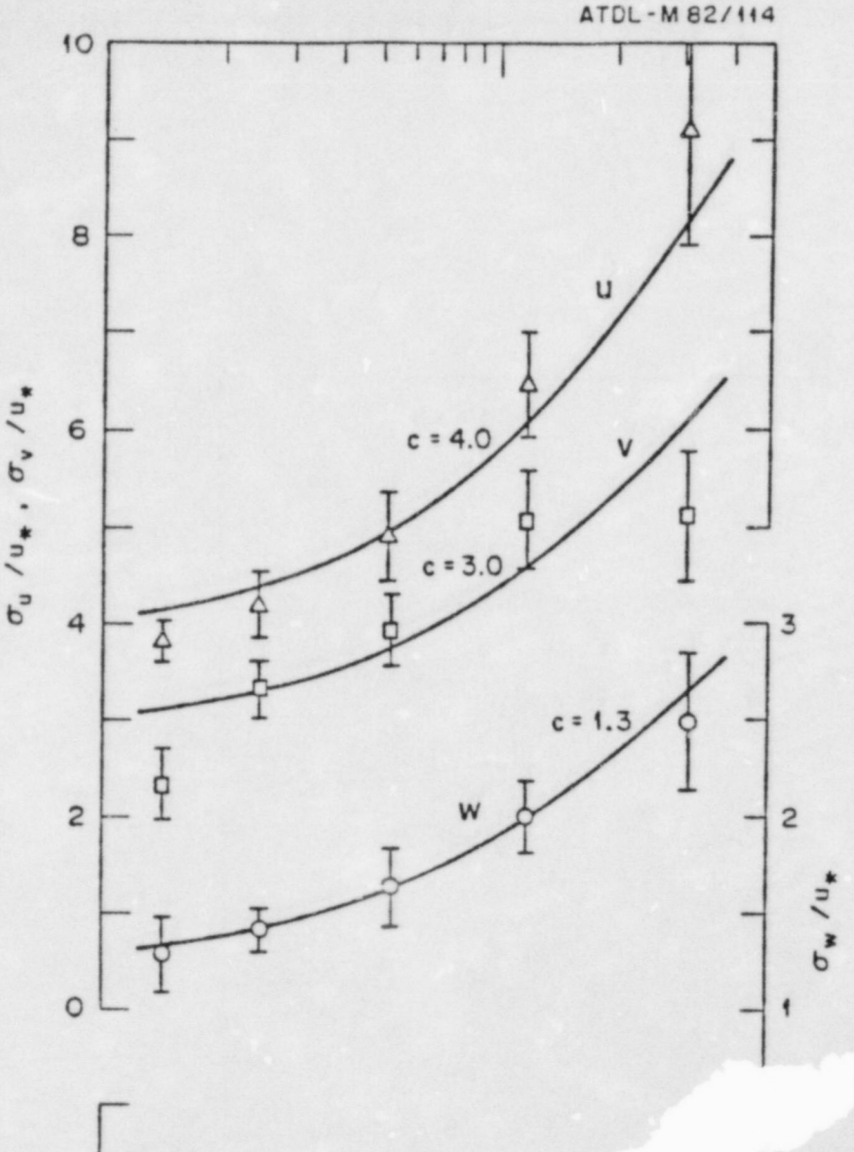

Figure 2 The apparent relationship between normalized turbulence statistics and stability, as generated by the inherent interdependence between the variables plotted. The raw "data" from which the graph was constructed were drawn from tables on random numbers. There is no relationship between the standard deviations and stability; the apparent order results solely from normalizing by the friction velocity. The curves drawn are from the published literature, all of the general form $\sigma/u_* = c(1 - az/L)^{1/3}$.

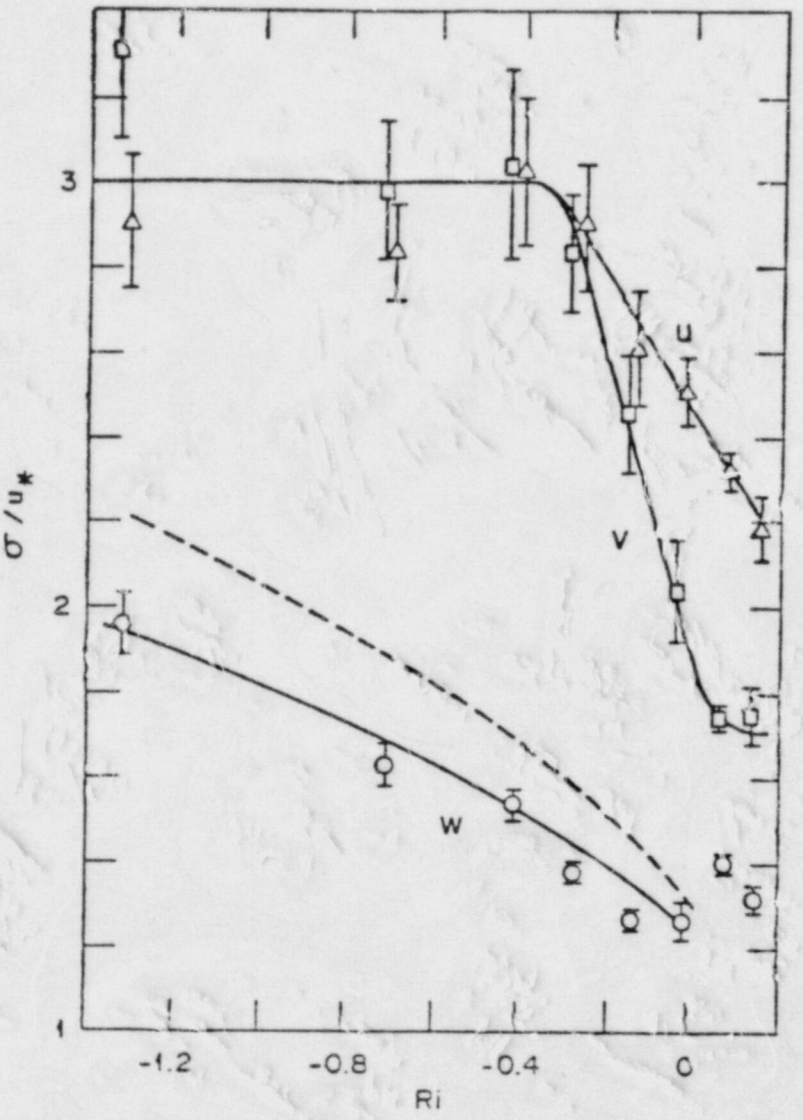

Figure 3 The variation with stability of the normalized velocity standard deviations for vertical (w, circles), lateral (v; squares) and longitudinal (u; triangles) wind fluctuations, derived from the Kansas data set (Izumi, 1971). The dashed line represents one of the most popular formulations, as represented in Figure 2, with a = 3 and with c = 1.3.

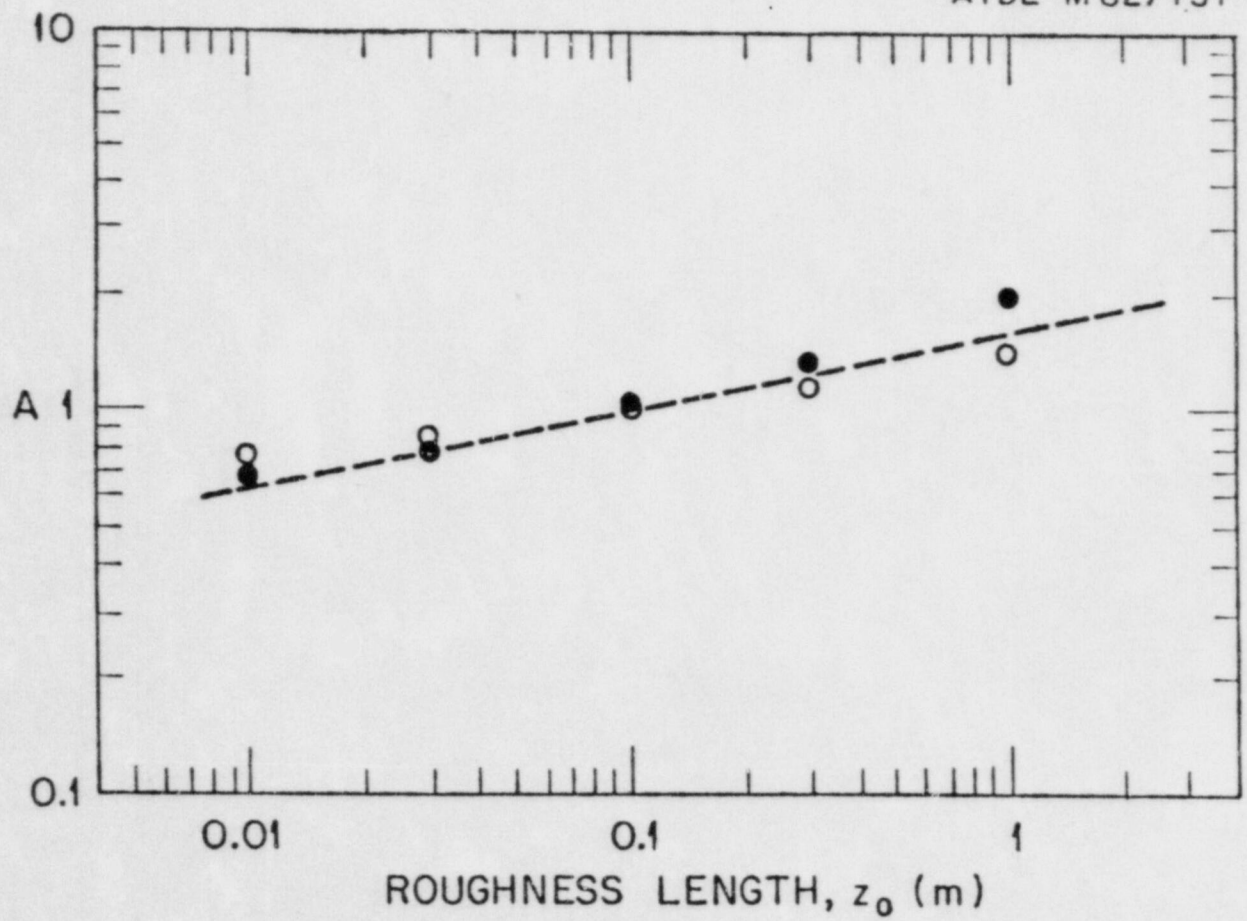

Figure 4 The effect of surface roughness length on vertical plume dispersion in the surface boundary layer, as specified by Eq. 4.12 for near-neutral conditions. The line drawn has a slope (corresponding to a power law exponent) of 0.2, as recommended by the American Meteorological Society 1977 Workshop on Stability Classification Schemes and Sigma Curves (see Hanna et al, 1977). The two sets of points plotted represent different assumptions regarding the height of observation, z = 10 m (o) and z = 300 m (•). However, note that the relations used to evaluate the ratio A are most accurate very near the surface.

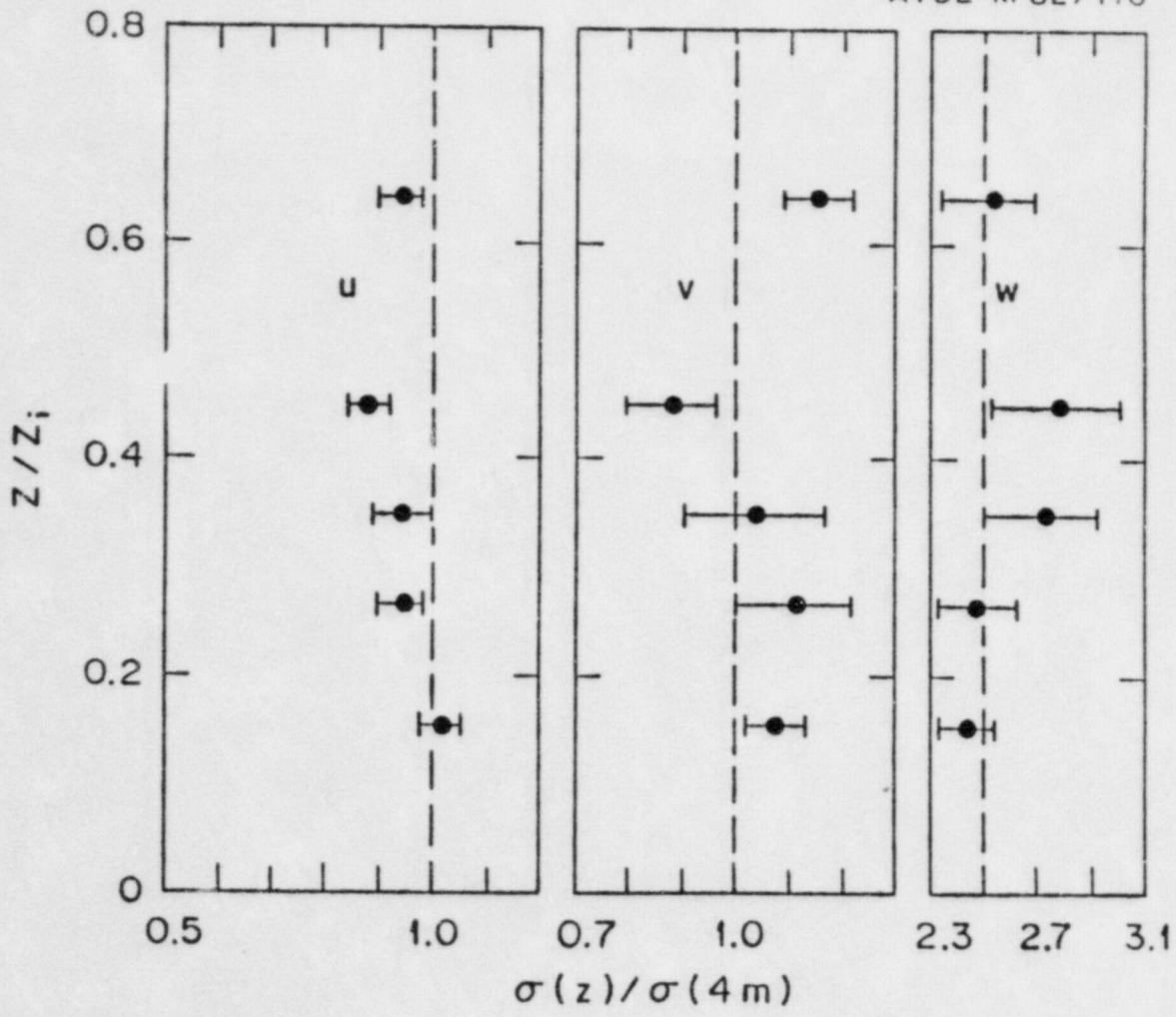

Figure 5 The variation with normalized height through the daytime mixed layer of the three velocity standard deviations, as derived from the 1973 Minnesota PBL experiment (Izumi and Caughey, 1976). Note that the standard deviations are normalized by simultaneous observations made at a constant 4 m height, and that the figure therefore represents a comparison between SBL and PBL turbulence behavior.

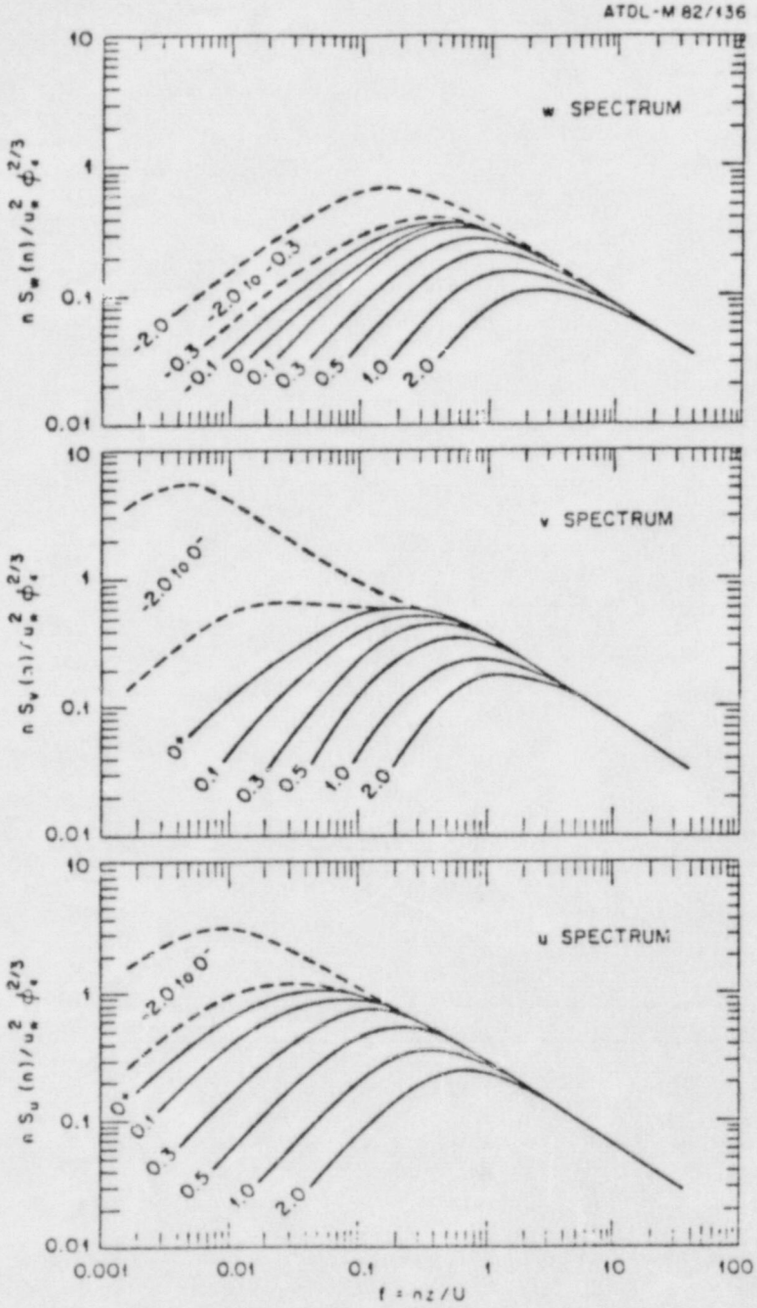

Figure 6 The variation with dimensionless frequency nz/U (where n is natural frequency) of the normalized spectral densities for vertical, transverse, and longitudinal velocity fluctuations, w, v, and u respectively. Curves are drawn to represent characteristic spectra for different atmospheric stabilities. Values of z/L are indicated. (From Kaimal el al., 1972).

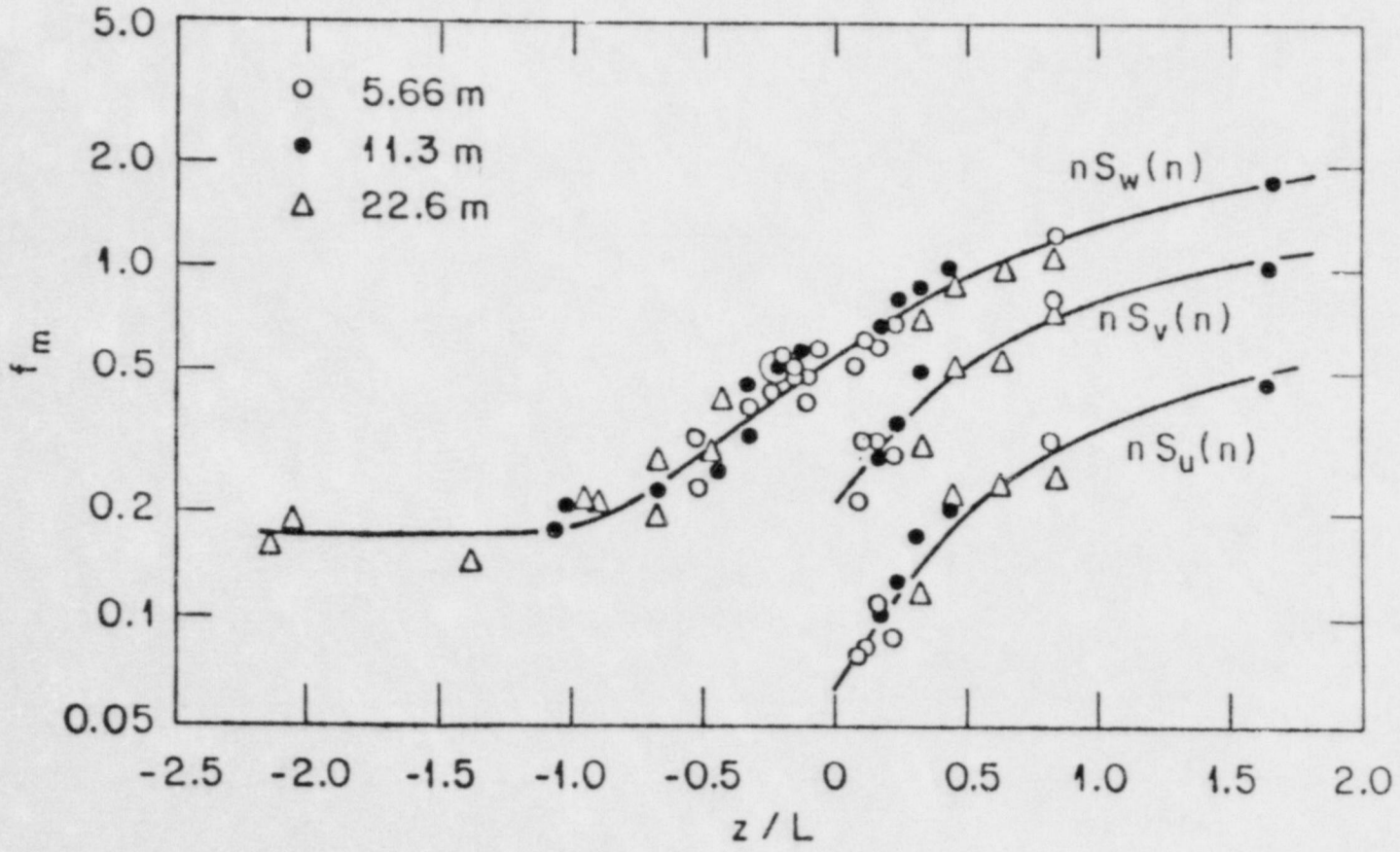

Figure 7 The variation with atmospheric stability z/L of the frequency (f_m) associated with the peak of the spectral density curves of Figure 6. (From Kaimal et al., 1972)

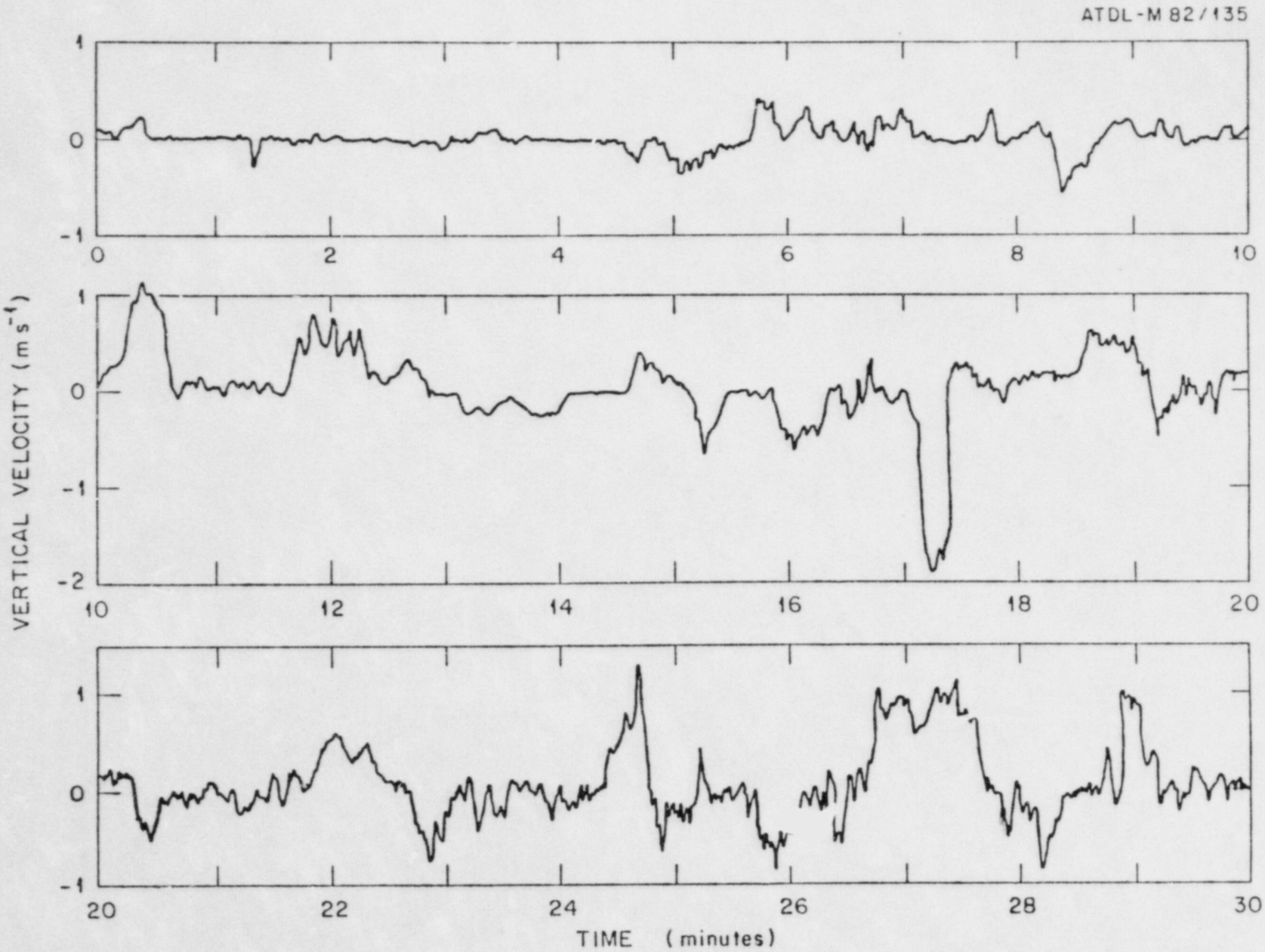

Figure 8 An example of a record of vertical velocity fluctuations, measured at about 10 m above the zero plane displacement of a deciduous forest.

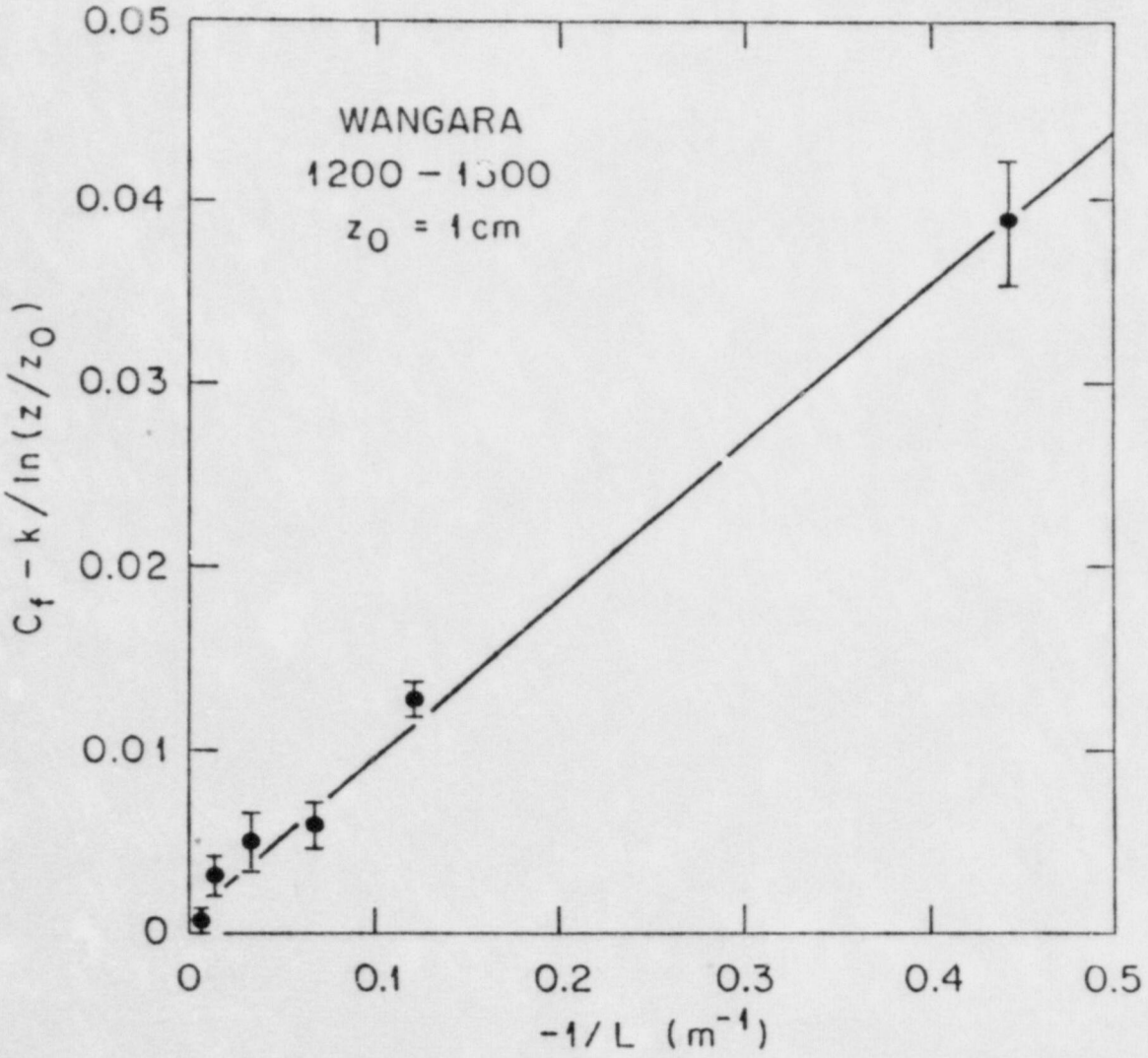

Figure 9 Friction coefficients in the unstable mixed layer as a function of the stability parameter -1/L. Note that the height dependence is contained within the logarithmic correction term in the ordinate. Data are for heights of 50, 100, 200, 500, and 1000 m, evaluated using a spatial average roughness length z_o = 1 cm.

NRC FORM 335 (11-81)

U.S. NUCLEAR REGULATORY COMMISSION

BIBLIOGRAPHIC DATA SHEET

1. REPORT NUMBER (Assigned by DDC)
NUREG/CR-3773

4. TITLE AND SUBTITLE (Add Volume No., if appropriate)
Variation of Planetary Boundary Layer Dispersion Properties with Height in Unstable Conditions

2. (Leave blank)

3. RECIPIENT'S ACCESSION NO.

7. AUTHOR(S)
B. B. Hicks

5. DATE REPORT COMPLETED
MONTH March YEAR 1984

9. PERFORMING ORGANIZATION NAME AND MAILING ADDRESS (Include Zip Code)
National Oceanic and Atmospheric Administration
Post Office Box E
Oak Ridge, Tennessee 37830

DATE REPORT ISSUED
MONTH May YEAR 1984

6. (Leave blank)

8. (Leave blank)

12. SPONSORING ORGANIZATION NAME AND MAILING ADDRESS (Include Zip Code)
Division of Radiation Programs and Earth Sciences
Office of Nuclear Regulatory Research
U.S. Nuclear Regulatory Commission
Washington, D.C. 20555

10. PROJECT/TASK/WORK UNIT NO.

11. FIN NO.
B6333

13. TYPE OF REPORT
Technical

PERIOD COVERED (Inclusive dates)

15. SUPPLEMENTARY NOTES

14. (Leave blank)

16. ABSTRACT (200 words or less)

Recent developments in surface boundary layer and planetary boundary layer meteorology are combined to evaluate the height dependency of the dispersion parameters σ_z and σ_y of the familiar Gaussian plume relationships. Recommendations are based on analyses of surface boundary layer data, such as are collected at industrial sites under existing NRC guidelines.

17. KEY WORDS AND DOCUMENT ANALYSIS

17a. DESCRIPTORS

Surface Boundary Layer
Planetary Boundary Layer
Dispersion
Meteorology

17b. IDENTIFIERS/OPEN-ENDED TERMS

18. AVAILABILITY STATEMENT
Unlimited

19. SECURITY CLASS (This report)
unclassified

21. NO. OF PAGES

20. SECURITY CLASS (This page)
unclassified

22. PRICE
$

NUREG/CR-3773

VARIATION OF PLANETARY BOUNDARY LAYER DISPERSION PROPERTIES WITH HEIGHT IN UNSTABLE CONDITIONS

MAY 1984